International Journal of Recent Technology and Engineering (IJRTE)
ISSN: 2277-3878 (Online), Volume-8 Issue-4, November 2019

# Differential Transform Technique on the Effect of Baffle Convective Nanofluid Flow in Saturated Porous Channel

**M. Karuna Prasad, J. Prathap Kumar, J.C. Umavathi, B. Devika, C. S. K. Raju**

***Abstract:*** ***Simulations are shown for steady nanofluid saturated with porous medium in a vertical channel divided into two way by placing a thin baffle. Tiwari and Das model applied for continuity, momentum and energy equations are written using to define the nanofluid and non-Darcy model used for porous medium. The nonlinear equations are solved analytically using regular perturbation method and by semi analytical method using differential transform method. The validity of the solutions obtained by perturbation method and differential transform method are compared and found that they agree very well for small values of perturbation parameters. The numerical values of the velocity and temperature are shown graphically at different baffle positions for all the pertinent parameters. The Nusselt number for both regular and nanofluids are evaluated and tabulated.***

***Keywords:*** ***Baffle, Differential Transform Technique, Nanofluid, Saturated Porous.***

## I. INTRODUCTION

Many young researchers are attracted in the area, the study of convection in a porous medium due to its practical applications in catalytic reactors, thermal insulation, oil and gas recovery, and including groundwater movement (Kaviany [1991], Nield and Bejan [2006]). If the velocity encountered is low, the Darcy equation can be used to describe the flow. However, the Darcy equation cannot account for the resistance caused by the solid boundaries. In order to account for viscous effects on confining boundaries, the Brinkman-extended Darcy equation is more appropriate and is usually integrated numerically. Various aspects for free convection porous flow between parallel plates (Kou and Lu [1993], Paul and Singh [1998], Al-Nimr and Hadded [1999] and Al- Nimr and Alkam [2000]) have been investigated. The effect of baffle on natural convection water based nanofluid under the impact of MHD is studied and observed optimum impact of baffle at base of the hot wall on heat transfer and enhancement in length of the baffle leads to enhance in heat transfer by Abedini [2018]. The practical applications are demonstrated by investigating the impact of continuous core baffle geometry on mixed convection heat transfer in heat exchangers and concluded continuous baffle can increase the energy efficiency in heat exchanger shell and coil and confirmed position of baffle influence a significant impact on heat transfer by Andrzejczyk and Muszynski [2018]. Investigated the impact of thin conducting baffle on buoyancy induced flow in a square cavity with asymmetric wall temperatures and observed that the length and position of the baffle impacts significantly to enhance the heat transfer compared with the wall without baffle by Tasnim and Collins [2004]. The thermal behavior of water based nanofluid in porous medium under the effect of uniform magnetic field and confined heat transfer is enhancing function of permeability and detracts with augment in Lorentz force and nanofluid is an increasing function of permeability by Sheikholeslami et. al. [2019]. Following the works mentioned above, we have analyzed the effect of baffle on mixed convection nanofluid flow in a vertical channel saturated with porous media using Robin boundary conditions.

Manuscript published on November 30, 2019.
* Correspondence Author
**Dr. Karuna Prasad***, Mathematics Department, GITAM (Deemed to be University), Bangalore, India. Email: karunaprasad9@gmail.com
**Prof. J. Prathap Kumar**, Mathematics Department, Gulbarga University, Kalaburagi, India. Email: p_rathap@yahoo.com
**Prof. J. C. Umavathi**, Mathematics Department, Gulbarga University, Kalaburagi, India. Email: drumavathi@rediffmail.com
**Dr. B. Devika**, Mathematics Department, GITAM (Deemed to be University), Bangalore, India. Email: devikamathematics@gmail.com.
**Dr. C. S. K. Raj,** Mathematics Department, GITAM (Deemed to be University), Bangalore, India. Email: sivaphd90@gmail.com

© The Authors. Published by Blue Eyes Intelligence Engineering and Sciences Publication (BEIESP). This is an open access article under the CC-BY-NC-ND license http://creativecommons.org/licenses/by-nc-nd/4.0/

## II. MATHEMATICAL FORMULATION

Analyzed geometrically, the steady fully developed, laminar nanofluid flow in a vertical parallel plate channel saturated by porous media as shown in Fig.1. The flow is disunited by placing a thin conducting negligible thickness baffle in the channel. The transverse velocity along Y-axis of vertical flow assumed negligible. Considered Copper, Silver, Diamond, Silicon Oxide and Titanium Oxide spherical shaped nanoparticles and water as a base fluid in thermal equilibrium. The momentum equations in both the streams along $X$ and $Y$ yield

Stream-I

$$(\rho\beta)_n g(T_1 - T_0) - \frac{\partial p}{\partial x} + \mu_n \frac{d^2 U_1}{dY^2} - \frac{\mu_n}{\kappa} U_1 = 0 \qquad (1)$$

Stream-II

$$(\rho\beta)_n g(T_2 - T_0) - \frac{\partial p}{\partial x} + \mu_n \frac{d^2 U_2}{dY^2} - \frac{\mu_n}{\kappa} U_2 = 0 \qquad (2)$$

where $\mu_n$, $\rho_n$, $\beta_n$ and $k_n$ are the viscosity, density, the coefficient of thermal expansion and thermal conductivity of the nanofluid, which are given by

$$\mu_n = \frac{\mu_b}{(1-\phi)^{2.5}},$$

$$(\rho\beta)_n = \rho_n\beta_n = (1-\phi)(\rho\beta)_b + (\rho\beta)_p\,\phi$$

$$k_n = k_b\left[\frac{k_p + 2k_b - 2\phi(k_b - k_p)}{k_p + 2k_p + \phi(k_b - k_p)}\right],$$

$$\rho_n = (1-\phi)\,\rho_b + \rho_p\phi.$$

Here $\mu_b$, $\rho_b$, $\beta_b$ and $k_b$ are the viscosity, density, the coefficient of thermal expansion and the thermal conductivity of the base fluid. $\mu_p$, $\rho_p$, $\beta_p$ and $k_p$ is the viscosity, density, the coefficient of thermal expansion and the thermal conductivity of solid particle.

The momentum balance equation along $Y$ in streams can be written as

$$\frac{\partial P}{\partial Y} = 0 \text{ where } P = p + \rho\, g\, X \tag{3}$$

the difference between the hydrostatic pressure and the pressure. Equation (3) holds that $P$ depends only on $X$. The pressure gradient in both the streams are assumed to be same.

The channel walls have negligible thickness and assumed the walls are exchanging the heat through convection with an outward fluid. Assumed that the fluid in both stream-I and stream-II have uniform reference temperatures $T_1$ and $T_2$ $(T_2 \geq T_1)$. $H_1$ and $H_2$ are the external convection coefficients at $Y = -l/2$ and at $Y = l/2$. Therefore, the temperature field boundary conditions can be expressed as

$$-k_n \left.\frac{\partial T_1}{\partial Y}\right|_{Y=-\frac{l}{2}} = H_1\left[T_1 - T(X, -l/2)\right] \tag{4}$$

$$-k_n \left.\frac{\partial T_2}{\partial Y}\right|_{Y=\frac{l}{2}} = H_2\left[T(X, l/2) - T_2\right] \tag{5}$$

The viscous dissipation energy balance equation yields

Stream-I

$$\frac{d^2T_1}{dY^2} = -\frac{\mu_b}{k_n}\left(\frac{dU_1}{dY}\right)^2 - \frac{\mu_b}{\kappa k_n}U_1^2 \tag{6}$$

Stream-II

$$\frac{d^2T_2}{dY^2} = -\frac{\mu_b}{k_n}\left(\frac{dU_2}{dY}\right)^2 - \frac{\mu_b}{\kappa k_n}U_2^2 \tag{7}$$

Eqns. (6) and (7) together with Eqns. (1) and (2) yield equations for velocity profile in both streams as follows

Stream-I

$$\frac{d^4U_1}{dY^4} = \frac{1}{\kappa}\frac{d^2U_1}{dY^2} + \frac{(\rho\beta)_n\,\mu_b g}{k_n\mu_n}\left(\frac{dU_1}{dY}\right)^2 + \frac{\mu_b(\rho\beta)_n\,g}{\kappa\mu_n}\frac{U_1^2}{k_n} \tag{8}$$

Stream-II

$$\frac{d^4U_2}{dY^4} = \frac{1}{\kappa}\frac{d^2U_2}{dY^2} + \frac{(\rho\beta)_n\,\mu_b g}{k_n\mu_n}\left(\frac{dU_2}{dY}\right)^2 + \frac{\mu_b(\rho\beta)_n\,g}{\kappa\mu_n}\frac{U_2^2}{k_n} \tag{9}$$

The stream-I and stream-II velocity boundary conditions are

$$U_1\left(-\frac{L}{2}\right) = U_2\left(\frac{L}{2}\right) = 0 \tag{10}$$

Eqns. (4) and (5), using eqns. (1) and (2) can be written as

$$\frac{d^3U_1}{dY^3} - \frac{h_1}{k_n}\frac{d^2U_1}{dY^2} - \frac{1}{\kappa}\frac{dU_1}{dY} + \frac{h_1}{k_n}\frac{1}{\kappa}U_1 = -\frac{h_1A}{\mu_n k_n} + \frac{h_1(\rho\beta)_n\,g}{\mu_n\kappa_n}[T_1 - T_0] \tag{11}$$

$$\frac{d^3U_2}{dY^3} + \frac{h_2}{k_n}\frac{d^2U_2}{dY^2} - \frac{1}{\kappa}\frac{dU_2}{dY} - \frac{h_2}{k_n}\frac{1}{\kappa}U_2 = \frac{h_2A}{\mu_n k_n} + \frac{h_2(\rho\beta)_n\,g}{\mu_n k_n}[T_0 - T_2] \tag{12}$$

where $\frac{dp}{dX} = A$

(13)

At the baffle position, the continuity of temperature and continuity of temperature gradients are considered as $(T_1 = T_2)$ and heat flux $\left(\frac{dT_1}{dY} = \frac{dT_2}{dY}\right)$. Using these conditions in Eqns. (1), (2), (6) and (7) yield

$$\frac{d^2U_1}{dY^2} = \frac{d^2U_2}{dY^2} \tag{14}$$

and

$$\frac{d^3U_1}{dY^3} - \frac{1}{\kappa}\frac{dU_1}{dY} = \frac{d^3U_2}{dY^3} - \frac{1}{\kappa}\frac{dU_2}{dY} \tag{15}$$

The velocity distribution with the boundary conditions of channel walls and at the baffle position represented by equations (8) and (9) are non-dimensionalized using the following dimensionless parameters:

$$u_i = \frac{U_i}{U_0}, y = \frac{Y}{D}, y^* = \frac{Y^*}{D^*}, Gr = \frac{g\beta_b\Delta T D^3}{\upsilon_b^2}, \mathrm{Re} = \frac{U_0 D}{\upsilon_b},$$

$$Br = \frac{U_0^2\mu_b}{k_b\Delta T}, \nu_b = \frac{\mu_b}{\rho_b}, \Lambda = \frac{Gr}{\mathrm{Re}}, \theta = \frac{T - T_0}{\Delta T}, Bi_1 = \frac{h_1 D}{k_b}, Bi_2 = \frac{h_2 D}{k_b}$$

$$S = \frac{Bi_1 Bi_2}{Bi_1 Bi_2 + 2Bi_1 + 2Bi_2}, \sigma = \frac{D}{\sqrt{\kappa}}, R_T = \frac{T_2 - T_1}{\Delta T}, I = \frac{C_f\, U_0 D^2}{\nu\sqrt{\kappa}} \tag{16}$$

In the above equation $D = 2L$ is the hydraulic diameter and the reference velocity and the reference temperature are given by

$$U_0 = -\frac{cD^2}{48\mu_b}, T_0 = \frac{T_1 + T_2}{2} + S\left(\frac{1}{Bi_1} - \frac{1}{Bi_2}\right)(T_2 - T_1) \tag{17}$$

The reference temperature $\Delta T$ is given either by

$$\Delta T = T_2 - T_1 \text{ if } T_1 < T_2 \tag{18}$$

or by

$$\Delta T = \frac{\mu_b^2}{\rho_b^2 C_p D^2} \text{ if } T_1 = T_2 \tag{19}$$

The non-dimension parameter $R_T = 1$ for asymmetric heating $(T_1 < T_2)$ and $R_T = 0$ for symmetric heating $(T_1 = T_2)$. By employing the dimensionless quantities as defined in Eqn. (16), Eqns. (8)-(15) can be written as

Stream-I

$$\frac{d^4u_1}{dy^4} - \sigma^2\frac{d^2u_1}{dy^2} = \Lambda\, Br\frac{c_2}{c_4}\left[\left(\frac{du_1}{dy}\right)^2 + c_1\sigma^2 u_1^2\right] \tag{20}$$

Stream-II

$$\frac{d^4u_2}{dy^4}-\sigma^2\frac{d^2u_2}{dy^2}=\Lambda\,Br\frac{c_2}{c_4}\left[\left(\frac{du_2}{dy}\right)^2+c_1\sigma^2{u_2}^2\right] \quad (21)$$

and the boundary conditions are

$$u_1=0,\ -\frac{1}{c_4}\frac{d^2u_1}{dy^2}+\frac{1}{Bi_1}\frac{d^3u_1}{dy^3}-\frac{\sigma^2}{Bi_1}\frac{du_1}{dy}=\frac{48c_1}{c_4}-\frac{c_1c_2}{c_4}\Lambda\frac{R_T}{2}S\left(1+\frac{4}{Bi_1}\right) \text{ : at } y=-\frac{1}{4}$$

$$u_2=0,\ \frac{1}{c_4}\frac{d^2u_2}{dy^2}+\frac{1}{Bi_2}\frac{d^3u_2}{dy^3}-\frac{\sigma^2}{Bi_2}\frac{du_2}{dy}=-\frac{48c_1}{c_4}-\frac{c_1c_2}{c_4}\Lambda\frac{R_T}{2}S\left(1+\frac{4}{Bi_2}\right) \text{ : at } y=\frac{1}{4}$$

and the boundary conditions are

$$u_1=0\ ;\ u_2=0;\ \frac{d^2u_1}{dy^2}=\frac{d^2u_2}{dy^2};$$

$$\frac{d^3u_1}{dy^3}-\sigma^2\frac{du_1}{dy}=\frac{d^3u_2}{dy^3}-\sigma^2\frac{du_2}{dy} \quad \text{at } y=y^* \quad (22)$$

where $c_1=(1-\phi)^{2.5}$, $c_2=\left[(1-\phi)+\frac{\phi(\rho\beta)_p}{(\rho\beta)_b}\right]$,

$c_3=\left[(1-\phi)+\frac{\phi(\rho)_p}{\rho_b}\right]$, $c_4=\left[\frac{k_p+2k_b-2\phi(k_b-k_p)}{k_p+2k_b+\phi(k_b-k_p)}\right]$

## III. SOLUTIONS

### A. Perturbation Method (PM)

The coupled nonlinear equations (20) and (21) are solved by using regular perturbation method. And this method strongly justified by considering small values of perturbation parameter $\varepsilon$ $(\varepsilon=\Lambda Br)$. By employing this technique, the approximate solutions of velocity profile obtained as in the form

$$u_i(y)=u_{i0}(y)+\varepsilon u_{i1}(y)+\varepsilon^2u_{i2}(y)+\ldots \quad (23)$$

Obtained the zeroth and first order equations by equating the coefficients of like power of $\varepsilon$ to zero and one in Eqns. (20), (21) and (22) using Eqn. (23).

Stream-I

Zeroth order equations

$$\frac{d^4u_{10}}{dy^4}-\sigma^2\frac{d^2u_{10}}{dy^2}=0 \quad (24)$$

First order equations

$$\frac{d^4u_{11}}{dy^4}=\sigma^2\frac{d^2u_{11}}{dy^2}+\frac{c_1c_2}{c_4}\sigma^2{u_{10}}^2+\frac{c_1c_2}{c_4}\left(\frac{du_{10}}{dy}\right)^2 \quad (25)$$

Stream-II

Zeroth order equations

$$\frac{d^4u_{20}}{dy^4}-\sigma^2\frac{d^2u_{20}}{dy^2}=0 \quad (26)$$

First order equations

$$\frac{d^4u_{21}}{dy^4}=\sigma^2\frac{d^2u_{21}}{dy^2}+\frac{c_1c_2}{c_4}\sigma^2{u_{20}}^2+\frac{c_1c_2}{c_4}\left(\frac{du_{20}}{dy}\right)^2 \quad (27)$$

The stream-I and stream-II corresponding boundary conditions are

Zeroth order

$$u_{10}=0,\frac{1}{Bi_1}\frac{d^3u_{10}}{dy^3}-\frac{1}{c_4}\frac{d^2u_{10}}{dy^2}-\frac{\sigma^2}{Bi_1}\frac{du_{10}}{dy}=Bc_1 \text{ at } y=-\frac{1}{4}$$

$$u_{20}=0,\frac{1}{Bi_2}\frac{d^3u_{20}}{dy^3}+\frac{1}{c_4}\frac{d^2u_{20}}{dy^2}-\frac{\sigma^2}{Bi_2}\frac{du_{20}}{dy}=Bc_2 \text{ at } y=\frac{1}{4}$$

$$u_{10}=0\ ;\ u_{20}=0\ ;\ \frac{d^2u_{10}}{dy^2}=\frac{d^2u_{20}}{dy^2}\ ;$$

$$\frac{d^3u_{10}}{dy^3}-\sigma^2\frac{du_{10}}{dy}=\frac{d^3u_{20}}{dy^3}-\sigma^2\frac{du_{20}}{dy} \text{ at } y=y^* \quad (28)$$

where

$$Bc_1=\frac{48c_1}{c_4}-\frac{c_1c_2}{c_4}\Lambda\frac{R_T}{2}S\left(1+\frac{4}{Bi_1}\right),\ Bc_2=-\frac{48c_1}{c_4}-\frac{c_1c_2}{c_4}\Lambda\frac{R_T}{2}S\left(1+\frac{4}{Bi_2}\right)$$

$$u_{11}=0;\frac{1}{Bi_1}\frac{d^3u_{11}}{dy^3}-\frac{1}{c_4}\frac{d^2u_{11}}{dy^2}-\frac{\sigma^2}{Bi_1}\frac{du_1}{dy}=0 \text{ at } y=-\frac{1}{4}$$

$$u_{21}=0,\ \frac{1}{Bi_2}\frac{d^3u_{21}}{dy^3}+\frac{1}{c_4}\frac{d^2u_{21}}{dy^2}-\frac{\sigma^2}{Bi_2}\frac{du_{21}}{dy}=0 \text{ at } y=\frac{1}{4}$$

$$u_{11}=0\ ;\ u_{21}=0\ ;\ \frac{d^2u_{11}}{dy^2}=\frac{d^2u_{21}}{dy^2}\ ;$$

$$\frac{d^3u_{11}}{dy^3}-\sigma^2\frac{du_{11}}{dy}=\frac{d^3u_{21}}{dy^3}-\sigma^2\frac{du_{21}}{dy} \text{ at } y=y^* \quad (29)$$

The solutions of zeroth and first order Eqns. (24)-(27) using the boundary conditions (28) and (29) are obtained.

Zeroth order

Stream-I

$$u_{10}=d_1+d_2y+d_3Cosh[\sigma y]+d_4Sinh[\sigma y] \quad (30)$$

Stream-II

$$u_{20}=d_5+d_6y+d_7Cosh[\sigma y]+d_8Sinh[\sigma y] \quad (31)$$

First order

Stream-I

$$u_{11}=c_3+c_4y+k_{10}y^2+k_{11}y^3+k_{01}y^4+k_{12}Cosh(\sigma y)+k_{13}Sinh(\sigma y)+k_{14}yCosh(\sigma y)+k_{15}ySinh(\sigma y)+k_{16}y^2Cosh(\sigma y)+k_{17}y^2Sinh(\sigma y)+k_{18}Cosh(2\sigma y)+k_{19}Sinh(2\sigma y) \quad (32)$$

Stream-II

$$u_{21}=c_7+c_8y+p_{10}y^2+p_{11}y^3+p_{01}y^4+p_{12}Cosh(\sigma y)+p_{13}Sinh(\sigma y)+p_{14}yCosh(\sigma y)+p_{15}ySinh(\sigma y)+p_{16}y^2Cosh(\sigma y)+p_{17}y^2Sinh(\sigma y)+p_{18}Cosh(2\sigma y)+p_{19}Sinh(2\sigma y) \quad (33)$$

Using the solutions of velocity fields Eqns. (1) and (2) yield

Stream-I

$$\theta_1=-1/\Lambda\left(\frac{48}{c_2}+\frac{\sigma^2}{c_1c_2}u_1+\frac{1}{c_1c_2}\frac{d^2u_1}{dy^2}\right) \quad (34)$$

Stream-II

$$\theta_2 = -\frac{1}{\Lambda}\left(\frac{48}{c_2} + \frac{\sigma^2}{c_1 E_2}u_2 + \frac{1}{c_1 c_2}\frac{d^2 u_2}{dy^2}\right) \quad (35)$$

where $u_1 = u_{10} + \varepsilon u_{11}$ *and* $u_2 = u_{20} + \varepsilon u_{21}$. (36)

The Nusselt number $Nu = \frac{d\theta}{dy}$ at both the walls are tabulated numerically for different values of some governing parameters and are given in Table-1.

(37)

(38)

## IV. RESULTS AND DISCUSSION

Mixed convection nanofluid flow in a vertical channel with the effect of baffle using Robin boundary conditions studied analytically by perturbation method and semi-analytically by differential transform method. The flow is disunited by placing a conducting thin baffle. The numerical values found for temperature and velocity fields for governing parameters such as mixed convection, porous, solid volume fraction, different nanoparticles and perturbation parameters for same and different Biot numbers are presented pictorially at different positions of the baffle. We considered water as base fluid and Copper as nanoparticle for all figures from 2 to 13 and all tables. Figures 2 and 3 exhibited the velocity and temperature fields for various estimations of permeable parameter for equivalent Biot numbers at various places of the baffle. Both the velocity field and temperature profile raise in Stream-I and diminishes in Stream-II when the baffle is set in center of the channel, and diminishes in the channel and increments close to the low heated wall when the baffle is situated close to the hot edge as increments in permeable parameter. The velocity field somewhat differs in Stream-I and diminishes in Stream-II, and temperature field increments in Stream-I and diminishes in Stream-II as increments in permeable parameter when the baffle is situated close to wall. It is observed from the figures 2 and 3 that both velocity and temperature increase gradually when compared to decreasing in the channel, this is occurred due to the effect of baffle and friction force of the porous matrix. Optimum value of the velocity profile raising as the baffle places shifting from hot wall to cold wall.

Figures 4 and 5 demonstrate the impact of mixed convection parameter on velocity and temperature fields for same Biot numbers and for different wall temperatures at various places of the baffle. $\varepsilon$ and $\Lambda$ are fixed as $\varepsilon = 0.1$ and $\Lambda = 500$ for upward flow $(\Lambda > 0)$, and $\varepsilon = -0.1$ and $\Lambda = -500$ for downward flow $(\Lambda < 0)$ for the figures 4 and 5. The velocity profile diminishes in left stream and raises in right stream for both ascending flow $(\Lambda > 0)$ and descending flow $(\Lambda < 0)$ as increments in $\Lambda$ at all places of the baffle is indicated in the Fig. 4. It is also seen from the Fig. 4 that optimum value of the velocity profile is occurred in a wider passage and it is in Stream-II for ascending flow $(\Lambda > 0)$ when the baffle is near the left wall, in Stream-I for descending flow $(\Lambda < 0)$ when the baffle is placed near the right wall and is symmetric when the baffle shifted to center of the channel as increases in $\Lambda$. The temperature raise in both the streams for both ascending and descending flow at all the baffle positions and it varies slightly in a narrow passage when compared to in a wider passage is observed from the Fig. 5.

The impact of $\sigma$ on velocity and temperature fields for different Biot numbers at various baffle places is shown in Fig. 6 and Fig. 7. Both the velocity and temperature fields diminish in both ways of the channel at all positions of the baffle but they are almost equal in Stream-I when the baffle is placed near the cold wall. The velocity reaches its optimum value in Stream-II when the baffle is positioned near the cold wall. Figures 8 and 9 show the effect of volume fraction of the nanoparticle on velocity and temperature fields for equal Biot numbers at different positions of the baffle. Figures 8 and 9 show the same situations of both velocity and temperature profiles as in figures 2 and 3 but in figures 8 and 9 the profiles of both velocity and temperature vary slightly when compared to figures 2 and 3 as increases in $\phi$. Figures 10 and 11 show the velocity and temperature profile for different values of $\phi$ for unequal Biot numbers at different baffle places. The velocity field increases in Stream-I and decreases in Stream-II as increases in $\phi$ at all places of the baffle is seen from the Fig.10. The temperature field increases in the channel but it slightly decreases near the hot wall as increases $\phi$ at all baffle places is seen from the Fig. 11.

Tables 2 to 13 show the effect of different nanoparticles ($N_p$) such as Copper (Cu), Diamond (Di), Silver (Ag), Titanium Oxide ($TiO_2$) and Silicon Oxide ($SiO_2$) on velocity and temperature profiles for equal and unequal Biot numbers at different positions of the baffle. For the tables 1 to 7 and figures 2, 3, 4, 5, 8 and 9, the governing parameters are fixed as $Bi_1 = 10,\ Bi_2 = 10,\ \Lambda = 500,\ \varepsilon = 0.1,\ \sigma = 4,\ R_T = 1$ *and* $\phi = 0.02$ and for the tables 8 to 13, and 6, 7, 10, 11, 12 and 13, the governing parameters are fixed a $Bi_1 = 1,\ Bi_2 = 10,\ \Lambda = 500,\ \varepsilon = 0.1,\ \sigma = 4,\ R_T = 1$ *and* $\phi = 0.02$ (except the varying parameter). The optimum value of the velocity profile is occurred in Stream-II for Silver nanoparticle when the baffle is placed near the cold wall and in middle of the channel, and is occurred in Stream-I for Diamond nanoparticle when the baffle is placed near the hot wall for both equal and unequal Biot numbers is observed from the figures 2, 3, 4, 8, 9 and 10. The optimum value of the temperature profile occurred for Silicon Oxide nanoparticle in Stream-II at all positions of the baffle for both equal and unequal Biot numbers is seen from the tables 5, 6, 7, 11, 12 and 13. Fig. 12 and

Fig.13 show the effect of $\varepsilon$ on the velocity and temperature fields for different positions of the baffle. The results obtained by using regular perturbation method are compared with the results obtained by using differential transform method with perturbation parameter. The results are agreed very well for small value $(\varepsilon < 1)$ of the perturbation parameter and the profiles are distinguished well for $(\varepsilon = 5)$ at all positions of the baffle, and both velocity and temperature profiles are increasing function of $\varepsilon$ is seen from the figures 12 and 13.

Table 1 shows the rate of heat transfer at both cold and hot wall for different values of governing parameters such as mixed convection parameter, Biot numbers, volume fraction of the nanoparticle, porous parameter and different nanoparticles at different positions of the baffle. The value of the Nusselt number increases at left wall and decreases at right wall as increases in $\Lambda$ at all places of the baffle, and it increases at both the walls at all the baffle positions as increases in Biot numbers and in porous parameter. The temperature gradient decreases at both cold wall and hot wall at all positions of the baffle as volume fraction of the nanoparticle increases. The optimum rate of heat transfer occurred at right wall for Silicon Oxide particles when the baffle is placed near the cold wall.

## A. Figures and Tables

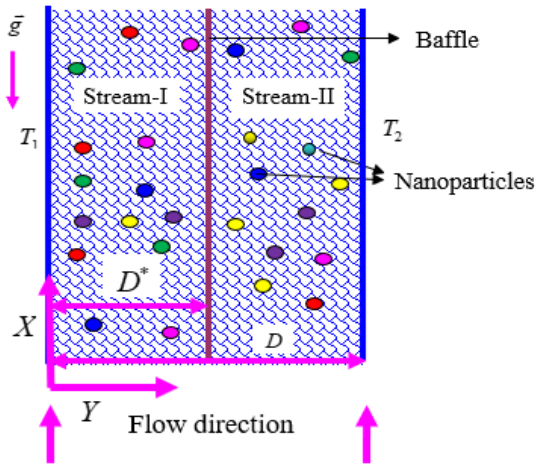


**Figure 1 Physical Model**

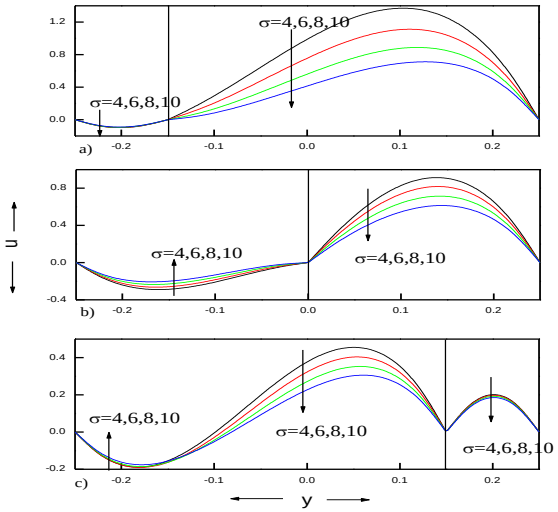


**Fig.2 Velocity profiles for different values of σ**

**a)**$y_b$=-0.15 b)$y_b$=0 c)$y_b$=0.15

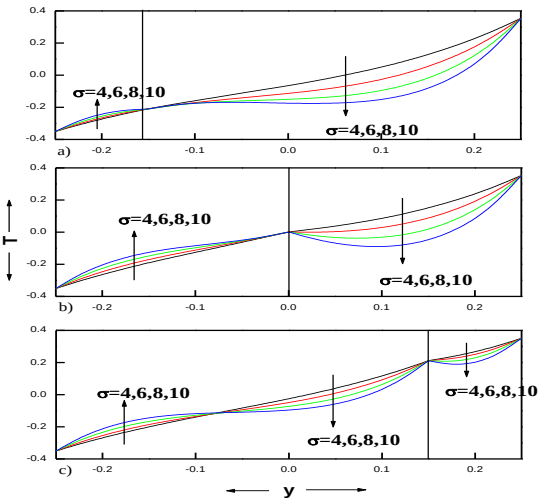


**Fig.3 Temperature profiles for different values of σ**

**a)**$y_b$=-0.15 b)$y_b$=0 c)$y_b$=0.15

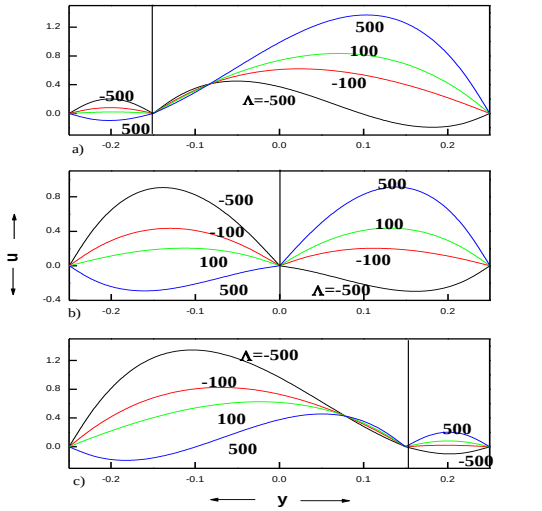


**Fig.4 Velocity profiles for different values of Λ**

**a)**$y_b$=-0.15 b)$y_b$=0 c)$y_b$=0.15

( ε=0.1 for +ve value of Λ &
ε=-0.1 for -ve value of Λ )

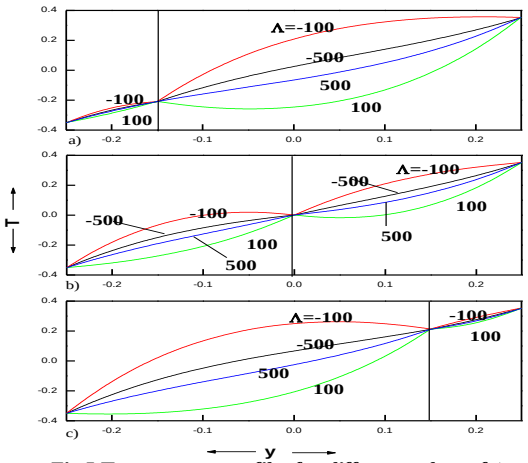


**Fig.5 Temperature profiles for different values of Λ**

**a)**$y_b$=-0.15 b)$y_b$=0 c)$y_b$=0.15

( ε=0.1 for +ve value of Λ &
ε=-0.1 for -ve value of Λ )

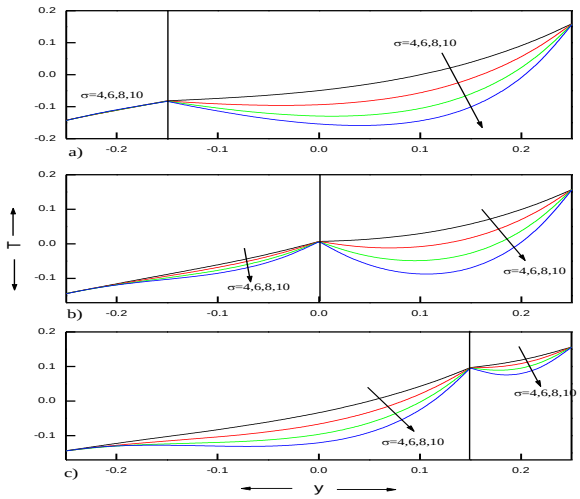


Fig.7 Temperature profiles for different values of σ
a)$y_b$=-0.15 b)$y_b$=0 c)$y_b$=0.15

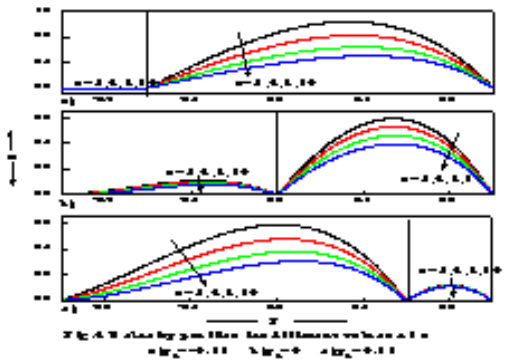

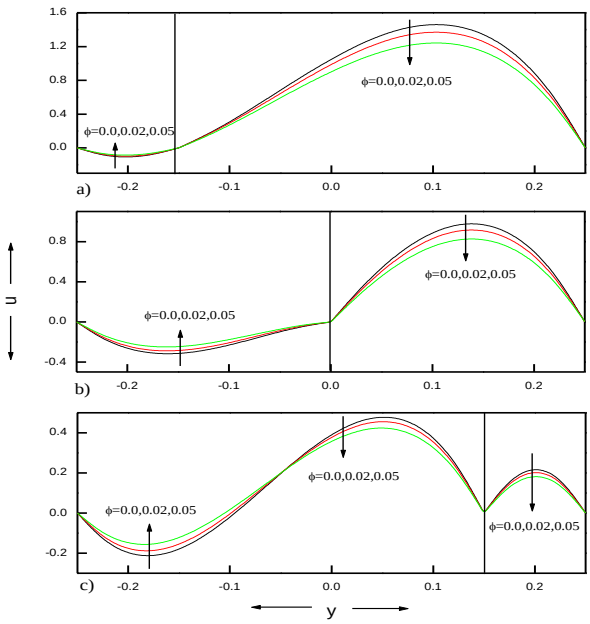


Fig.8 Velocity profiles for different values of ϕ
a)$y_b$=-0.15 b)$y_b$=0 c)$y_b$=0.15

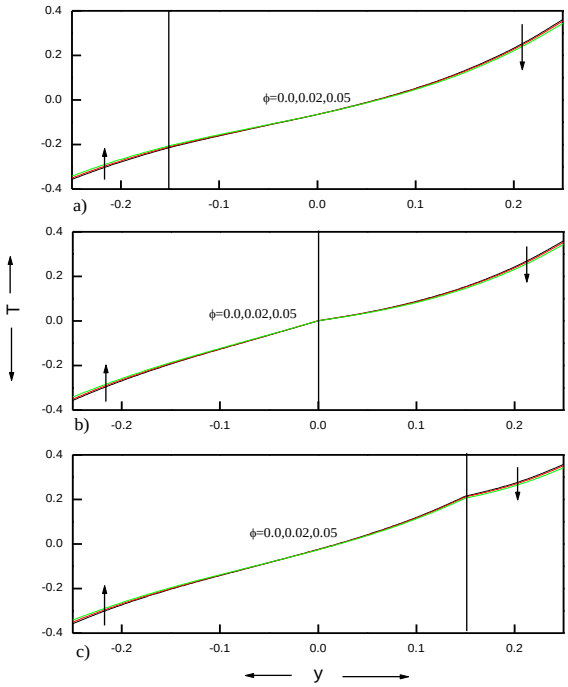


Fig.9 Temperature profiles for different values of ϕ
a)$y_b$=-0.15 b)$y_b$=0 c)$y_b$=0.15

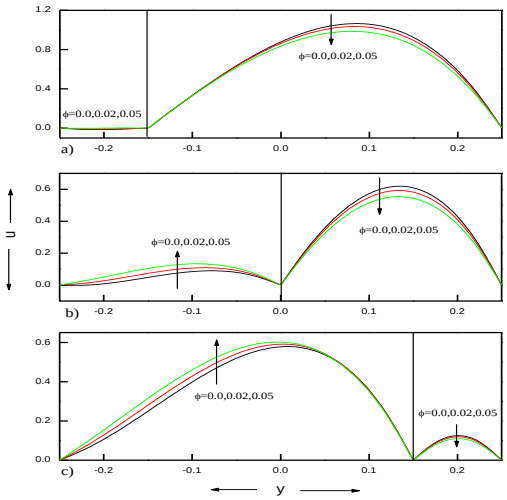


Fig.10 Velocity profiles for different values of ϕ
a)$y_b$=-0.15 b)$y_b$=0 c)$y_b$=0.15

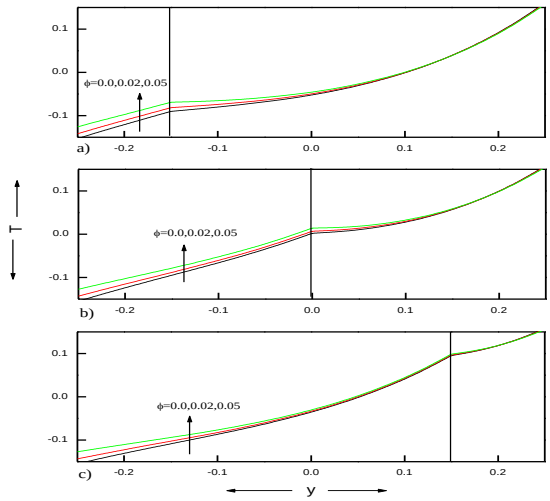


Fig.11 Temperature profiles for different values of ϕ
a)$y_b$=-0.15 b)$y_b$=0 c)$y_b$=0.15

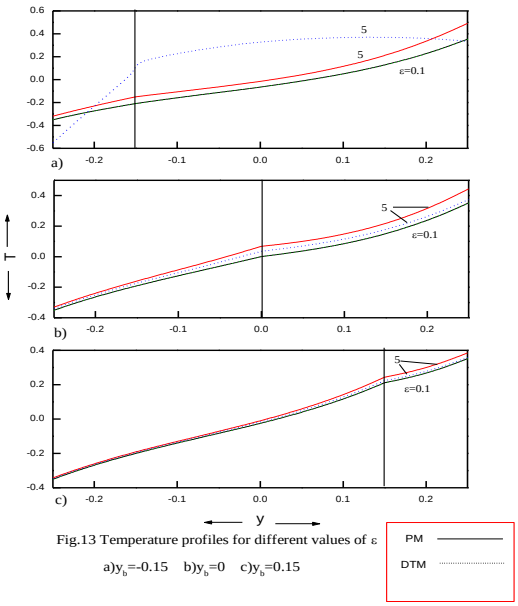


Fig.13 Temperature profiles for different values of ε
a)$y_b$=-0.15 b)$y_b$=0 c)$y_b$=0.15

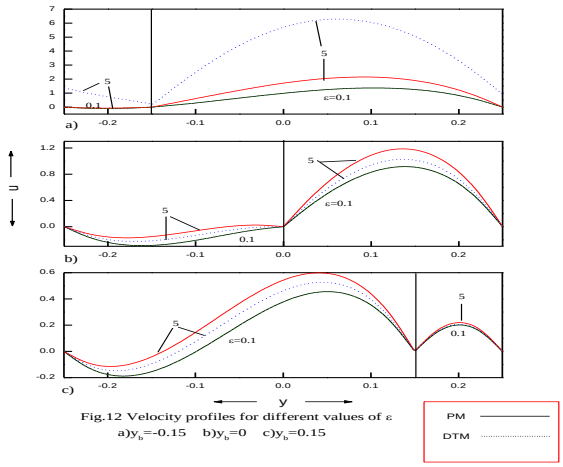


Fig.12 Velocity profiles for different values of ε
a)$y_b$=-0.15 b)$y_b$=0 c)$y_b$=0.15

**Table -I**

| | $\left(\frac{d\theta}{dy}\right)_{y=-\frac{1}{4}}$ | | | $\left(\frac{d\theta}{dy}\right)_{y=\frac{1}{4}}$ | | |
|---|---|---|---|---|---|---|
| | $Y_b$=-0.15 | $Y_b$=0 | $Y_b$=0.15 | $Y_b$=-0.15 | $Y_b$=0 | $Y_b$=0.15 |
| $\Lambda$ | | | | | | |
| 100 | 1.13134 | 0.50090 | -0.21185 | 4.93701 | 4.07483 | 2.65020 |
| 250 | 1.58518 | 1.57066 | 1.32634 | 3.39109 | 3.00232 | 2.19104 |
| 500 | 1.73714 | 1.92774 | 1.83916 | 2.87760 | 2.64634 | 2.03830 |
| $Bi_1$ | | | | | | |
| 1 | 0.64626 | 0.59500 | 0.45887 | 1.56539 | 1.35850 | 0.96805 |
| 5 | 1.48764 | 1.62155 | 1.52103 | 2.58625 | 2.35909 | 1.79770 |
| 10 | 1.73714 | 1.92774 | 1.83916 | 2.87760 | 2.64634 | 2.03830 |
| $Bi_2$ | | | | | | |
| 1 | 0.66259 | 0.63795 | 0.51936 | 1.49356 | 1.31441 | 0.94971 |
| 5 | 1.49555 | 1.63999 | 1.54659 | 2.55754 | 2.34014 | 1.79000 |
| 10 | 1.73714 | 1.92774 | 1.83916 | 2.87760 | 2.64634 | 2.03830 |
| $\phi$ | | | | | | |
| 0.0 | 1.77177 | 1.96977 | 1.88285 | 2.91818 | 2.68542 | 2.07049 |
| 0.02 | 1.73714 | 1.92774 | 1.83916 | 2.87760 | 2.64634 | 2.03830 |
| 0.05 | 1.68515 | 1.86437 | 1.77316 | 2.81699 | 2.58768 | 1.98972 |
| $\sigma$ | | | | | | |
| 4 | 1.73714 | 1.92774 | 1.83916 | 2.87760 | 2.64634 | 2.03830 |

| | | | | | | |
|---|---|---|---|---|---|---|
| 6 | 2.13472 | 2.51275 | 2.37343 | 4.32663 | 3.99728 | 2.80912 |
| 8 | 2.67344 | 3.24226 | 3.08036 | 5.95480 | 5.61510 | 3.84976 |
| 10 | 3.33694 | 4.06906 | 3.91142 | 7.66388 | 7.36998 | 5.12678 |
| $N_p$ | | | | | | |
| Cu | 1.73714 | 1.92774 | 1.83916 | 2.87760 | 2.64634 | 2.03830 |
| Di | 1.73474 | 1.92236 | 1.83153 | 2.88480 | 2.65133 | 2.04043 |
| Ag | 1.73770 | 1.92902 | 1.84100 | 2.87579 | 2.64508 | 2.03774 |
| $TiO_2$ | 1.74068 | 1.92946 | 1.83877 | 2.89245 | 2.65866 | 2.04639 |
| $SiO_2$ | 1.76014 | 1.95305 | 1.86314 | 2.91609 | 2.68157 | 2.06529 |

**Table-2: Values of velocity field for different values of $N_p$ at $y_b$=-0.15**

| y | Cu | Di | Ag | $TiO_2$ | $SiO_2$ |
|---|---|---|---|---|---|
| -0.25 | 0 | 0 | 0 | 0 | 0 |
| -0.2 | -0.10662 | -0.10427 | -0.10721 | -0.10473 | -0.10652 |
| -0.15 | 0 | 0 | 0 | 0 | 0 |
| -0.1 | 0.29135 | 0.29173 | 0.29126 | 0.29168 | 0.29147 |
| -0.05 | 0.64469 | 0.64309 | 0.64509 | 0.64344 | 0.64481 |
| 0 | 0.99061 | 0.98583 | 0.9918 | 0.98681 | 0.99066 |
| 0.05 | 1.25944 | 1.25135 | 1.26145 | 1.25299 | 1.25938 |
| 0.1 | 1.37844 | 1.36802 | 1.38104 | 1.37011 | 1.37829 |
| 0.15 | 1.2689 | 1.25822 | 1.27156 | 1.26035 | 1.26869 |
| 0.2 | 0.84293 | 0.83528 | 0.84484 | 0.8368 | 0.84276 |
| 0.25 | 0 | 0 | 0 | 0 | 0 |

**Table-3: Values of temperature field for different values of Np at yb= 0**

| y | Cu | Di | Ag | $TiO_2$ | $SiO_2$ |
|---|---|---|---|---|---|
| -0.25 | 0 | 0 | 0 | 0 | 0 |
| -0.2 | -0.2496 | -0.24305 | -0.2513 | -0.24433 | -0.24936 |
| -0.15 | -0.2914 | -0.28278 | -0.2936 | -0.28446 | -0.29106 |
| -0.1 | -0.2105 | -0.20307 | -0.2124 | -0.20452 | -0.21021 |
| -0.05 | -0.0872 | -0.08299 | -0.0882 | -0.08381 | -0.08702 |
| 0 | 0 | 0 | 0 | 0 | 0 |
| 0.05 | 0.50917 | 0.50474 | 0.51028 | 0.50561 | 0.50905 |
| 0.1 | 0.83924 | 0.83146 | 0.84118 | 0.83299 | 0.83902 |
| 0.15 | 0.92004 | 0.91108 | 0.92227 | 0.91285 | 0.91977 |
| 0.2 | 0.67141 | 0.66461 | 0.6731 | 0.66595 | 0.6712 |
| 0.25 | 0 | 0 | 0 | 0 | 0 |

**Table-4: Values velocity field for different values of Np at yb= 0.15**

| y | Cu | Di | Ag | $TiO_2$ | $SiO_2$ |
|---|---|---|---|---|---|
| -0.25 | 0 | 0 | 0 | 0 | 0 |
| -0.2 | -0.18537 | -0.17801 | -0.1872 | -0.17943 | -0.18505 |
| -0.15 | -0.15987 | -0.14966 | -0.1624 | -0.15164 | -0.15942 |
| -0.1 | -0.00583 | 0.00402 | -0.0082 | 0.00211 | -0.00538 |
| -0.05 | 0.19957 | 0.20706 | 0.1977 | 0.20561 | 0.19993 |
| 0 | 0.38122 | 0.38546 | 0.38017 | 0.38465 | 0.38145 |
| 0.05 | 0.46308 | 0.46425 | 0.46279 | 0.46403 | 0.46317 |
| 0.1 | 0.3651 | 0.36447 | 0.36525 | 0.3646 | 0.3651 |
| 0.15 | 0 | 0 | 0 | 0 | 0 |
| 0.2 | 0.21977 | 0.21739 | 0.22037 | 0.21786 | 0.21968 |
| 0.25 | 0 | 0 | 0 | 0 | 0 |

**Table-5: Values of temperature field for different values of Np at yb= -0.15**

| y | Cu | Di | Ag | $TiO_2$ | $SiO_2$ |
|---|---|---|---|---|---|
| -0.25 | -0.35040 | -0.35039 | -0.3504 | -0.3514 | -0.3550 |
| -0.2 | -0.27268 | -0.27274 | -0.2726 | -0.2735 | -0.2762 |
| -0.15 | -0.2094 | -0.20941 | -0.2093 | -0.2100 | -0.2121 |
| -0.1 | -0.15863 | -0.15896 | -0.1585 | -0.1593 | -0.1607 |
| -0.05 | -0.11207 | -0.11262 | -0.1119 | -0.1128 | -0.1135 |
| 0 | -0.06503 | -0.06572 | -0.0648 | -0.0657 | -0.0659 |
| 0.05 | -0.01281 | -0.01354 | -0.0126 | -0.0134 | -0.0129 |
| 0.1 | 0.04954 | 0.04884 | 0.04971 | 0.0491 | 0.0501 |
| 0.15 | 0.12733 | 0.12676 | 0.12747 | 0.1272 | 0.1290 |
| 0.2 | 0.22652 | 0.22615 | 0.2266 | 0.2269 | 0.2295 |
| 0.25 | 0.35383 | 0.35377 | 0.35384 | 0.3549 | 0.3585 |

**Table-6: Values of temperature field for different values of Np at yb= 0**

| y | Cu | Di | Ag | $TiO_2$ | $SiO_2$ |
|---|---|---|---|---|---|
| -0.25 | -0.3506 | -0.3505 | -0.3506 | -0.35169 | -0.3552 |
| -0.2 | -0.26331 | -0.2635 | -0.26325 | -0.2643 | -0.2667 |
| -0.15 | -0.19008 | -0.1904 | -0.19 | -0.19093 | -0.1926 |
| -0.1 | -0.12516 | -0.1254 | -0.12508 | -0.12581 | -0.1268 |
| -0.05 | -0.06312 | -0.0633 | -0.06306 | -0.0635 | -0.0639 |
| 0 | 0.00136 | 0.00134 | 0.00137 | 0.00135 | 0.0014 |
| 0.05 | 0.03727 | 0.03703 | 0.03733 | 0.0372 | 0.03777 |
| 0.1 | 0.08526 | 0.08492 | 0.08534 | 0.08525 | 0.08639 |
| 0.15 | 0.1501 | 0.14975 | 0.15018 | 0.15029 | 0.15209 |
| 0.2 | 0.23722 | 0.23697 | 0.23728 | 0.23777 | 0.24037 |
| 0.25 | 0.35291 | 0.35285 | 0.35292 | 0.35397 | 0.3576 |

**Table-7: Values of temperature field for different values of Np at yb= 0.15**

| y | Cu | Di | Ag | $TiO_2$ | $SiO_2$ |
|---|---|---|---|---|---|
| -0.25 | -0.3508 | -0.35084 | -0.3508 | -0.35194 | -0.35548 |
| -0.2 | -0.2680 | -0.26834 | -0.2679 | -0.26912 | -0.27157 |
| -0.15 | -0.1994 | -0.20001 | -0.1993 | -0.20053 | -0.20212 |
| -0.1 | -0.1396 | -0.14029 | -0.1394 | -0.14059 | -0.14148 |
| -0.05 | -0.0832 | -0.08396 | -0.0830 | -0.08408 | -0.08437 |
| 0 | -0.0252 | -0.02595 | -0.0251 | -0.02589 | -0.02563 |
| 0.05 | 0.03945 | 0.0389 | 0.03958 | 0.03913 | 0.03995 |
| 0.1 | 0.11634 | 0.116 | 0.11642 | 0.11643 | 0.11787 |
| 0.15 | 0.21129 | 0.21127 | 0.21129 | 0.21194 | 0.21409 |
| 0.2 | 0.26664 | 0.26656 | 0.26665 | 0.26741 | 0.27016 |
| 0.25 | 0.35172 | 0.35169 | 0.35172 | 0.3528 | 0.35637 |

**Table-8: Values of velocity field for different values of Np at yb= -0.15**

| y | Cu | Di | Ag | $TiO_2$ | $SiO_2$ |
|---|---|---|---|---|---|
| -0.25 | 0 | 0 | 0 | 0 | 0 |
| -0.2 | -0.0087 | -0.0078 | -0.0089 | -0.0088 | -0.0123 |
| -0.15 | 0 | 0 | 0 | 0 | 0 |
| -0.1 | 0.33708 | 0.33683 | 0.33716 | 0.33361 | 0.32308 |
| -0.05 | 0.63408 | 0.6327 | 0.63445 | 0.62773 | 0.61161 |
| 0 | 0.86721 | 0.8643 | 0.86797 | 0.85872 | 0.84082 |
| 0.05 | 1.01013 | 1.00575 | 1.01125 | 1.00044 | 0.98361 |
| 0.1 | 1.03289 | 1.02756 | 1.03425 | 1.02315 | 1.00939 |
| 0.15 | 0.90074 | 0.89547 | 0.90207 | 0.89236 | 0.88292 |
| 0.2 | 0.57271 | 0.56902 | 0.57364 | 0.56745 | 0.56282 |
| 0.25 | 0 | 0 | 0 | 0 | 0 |

**Table-9: Values of velocity field for different values of Np at yb= 0**

| y | Cu | Di | Ag | $TiO_2$ | $SiO_2$ |
|---|---|---|---|---|---|
| -0.25 | 0 | 0 | 0 | 0 | 0 |
| -0.2 | 0.0265 | 0.02914 | 0.02586 | 0.02581 | 0.01452 |
| -0.15 | 0.07391 | 0.07734 | 0.07308 | 0.07262 | 0.05665 |
| -0.1 | 0.10846 | 0.11138 | 0.10775 | 0.1069 | 0.0918 |
| -0.05 | 0.09588 | 0.0975 | 0.09549 | 0.09466 | 0.0851 |
| 0 | 0 | 0 | 0 | 0 | 0 |
| 0.05 | 0.35059 | 0.3485 | 0.35112 | 0.34745 | 0.34427 |
| 0.1 | 0.55682 | 0.5532 | 0.55773 | 0.55187 | 0.548 |
| 0.15 | 0.59132 | 0.5872 | 0.59236 | 0.58611 | 0.58311 |
| 0.2 | 0.41988 | 0.41678 | 0.42066 | 0.41621 | 0.41477 |
| 0.25 | 0 | 0 | 0 | 0 | 0 |

**Table-10: Values of velocity field for different values of $N_p$ at $y_b$= 0.15**

| Values of velocity field for different values of $N_p$ at $y_b$= 0.15 | | | | | |
|---|---|---|---|---|---|
| y | Cu | Di | Ag | $TiO_2$ | $SiO_2$ |
| -0.25 | 0 | 0 | 0 | 0 | 0 |
| -0.2 | 0.12772 | 0.13063 | 0.12702 | 0.12601 | 0.11043 |
| -0.15 | 0.28079 | 0.28475 | 0.27984 | 0.27741 | 0.25277 |
| -0.1 | 0.42971 | 0.43342 | 0.42883 | 0.42490 | 0.39645 |
| -0.05 | 0.54484 | 0.54749 | 0.54422 | 0.53905 | 0.51100 |
| 0 | 0.59515 | 0.59645 | 0.59487 | 0.58909 | 0.56477 |
| 0.05 | 0.54706 | 0.54714 | 0.54707 | 0.54166 | 0.52367 |
| 0.1 | 0.36301 | 0.36249 | 0.36315 | 0.35951 | 0.34982 |
| 0.15 | 0 | 0 | 0 | 0 | 0 |
| 0.2 | 0.12974 | 0.12868 | 0.13001 | 0.12863 | 0.12863 |
| 0.25 | 0 | 0 | 0 | 0 | 0 |

**Table-11: Values of temperature field for different values of Np at yb= -0.15**

| y | Cu | Di | Ag | $TiO_2$ | $SiO_2$ |
|---|---|---|---|---|---|
| -0.25 | -0.1417 | -0.1417 | -0.1417 | -0.1437 | -0.1504 |
| -0.2 | -0.1109 | -0.1110 | -0.1109 | -0.1128 | -0.1185 |
| -0.15 | -0.0814 | -0.0814 | -0.0814 | -0.0830 | -0.0883 |
| -0.1 | -0.0741 | -0.0744 | -0.0740 | -0.0756 | -0.0793 |
| -0.05 | -0.0641 | -0.0646 | -0.0639 | -0.0654 | -0.0681 |
| 0 | -0.0498 | -0.0504 | -0.0496 | -0.0510 | -0.0528 |
| 0.05 | -0.0293 | -0.0301 | -0.0292 | -0.0304 | -0.0315 |
| 0.1 | -0.0008 | -0.0015 | -0.0006 | -0.0017 | -0.0023 |
| 0.15 | 0.03816 | 0.03759 | 0.03830 | 0.03752 | 0.03736 |
| 0.2 | 0.0904 | 0.09005 | 0.09049 | 0.0901 | 0.09032 |
| 0.25 | 0.15917 | 0.15913 | 0.15918 | 0.15931 | 0.15989 |

**Table-12: Values of temperature field for different values of Np at yb= 0**

| y | Cu | Di | Ag | $TiO_2$ | $SiO_2$ |
|---|---|---|---|---|---|
| -0.25 | -0.1433 | -0.1432 | -0.14329 | -0.14531 | -0.1519 |
| -0.2 | -0.1150 | -0.1152 | -0.11497 | -0.1168 | -0.1219 |
| -0.15 | -0.0881 | -0.0884 | -0.08809 | -0.08973 | -0.0938 |
| -0.1 | -0.0604 | -0.0607 | -0.06036 | -0.06181 | -0.0652 |
| -0.05 | -0.0295 | -0.0297 | -0.02947 | -0.03068 | -0.0337 |
| 0 | 0.00702 | 0.00702 | 0.00703 | 0.0061 | 0.0031 |
| 0.05 | 0.01335 | 0.01313 | 0.0134 | 0.0125 | 0.01048 |
| 0.1 | 0.02942 | 0.0291 | 0.02951 | 0.02871 | 0.02748 |
| 0.15 | 0.05712 | 0.05679 | 0.0572 | 0.05661 | 0.05605 |
| 0.2 | 0.09874 | 0.09852 | 0.0988 | 0.09852 | 0.09857 |
| 0.25 | 0.15716 | 0.15713 | 0.15717 | 0.15733 | 0.15797 |

**Table-13: Values of temperature field for different values of $N_p$ at $y_b$= 0.15**

| y | Cu | Di | Ag | $TiO_2$ | $SiO_2$ |
|---|---|---|---|---|---|
| -0.25 | -0.1436 | -0.1435 | -0.1436 | -0.14562 | -0.1523 |
| -0.2 | -0.1222 | -0.1225 | -0.12212 | -0.124 | -0.1288 |
| -0.15 | -0.1025 | -0.1030 | -0.10238 | -0.10414 | -0.1076 |
| -0.1 | -0.0825 | -0.0832 | -0.08239 | -0.08401 | -0.0865 |
| -0.05 | -0.0603 | -0.0610 | -0.06013 | -0.0616 | -0.0634 |
| 0 | -0.0336 | -0.0343 | -0.03351 | -0.03478 | -0.0361 |
| 0.05 | -0.0003 | -0.0009 | -0.0002 | -0.00128 | -0.0023 |
| 0.1 | 0.04209 | 0.04177 | 0.04216 | 0.04148 | 0.04056 |
| 0.15 | 0.09666 | 0.09666 | 0.09666 | 0.0964 | 0.09552 |
| 0.2 | 0.11787 | 0.11782 | 0.11789 | 0.11777 | 0.11763 |
| 0.25 | 0.15664 | 0.15664 | 0.15664 | 0.15681 | 0.15739 |

## REFERENCES

1. M. Kaviany, Principles of heat transfer in porous media, Springer, New York, 1991.
2. D. A. Nield, and A. Bejan, Convection in porous media, 3rd Edition, Springer-Varlag, New York, 2006.
3. H. S. Kou and K. T. Lu, "Combined boundary and inertia effects for fully developed mixed convection in a vertical channel imbedded in a porous media", Int. Commun. Heat and Mass Transfer, Vol. 20, 1993, pp. 333-345.
4. T. Paul and A. K. Singh, "Natural convection between coaxial vertical cylinders partially filled with porous material", Eng. Res., Vol. 64, 1998, pp. 157-162.
5. M. A. Al-Nimr and O. M. Haddad, "Fully developed free convection in open ended vertical channels partially filled with porous material, J. Porous Media, Vol. 2, 1999, pp. 179-189.

6. M. A. Al-Nimr and M. K. Alkam, “Basic fluid flow problems in porous media”, J. Porous Media, Vol. 3, 2000, pp. 45-49.
7. S. U. S. Choi, “Enhancing thermal conductivity of fluids with nanoparticles”, Developments and Applications of Non-Newtonian Flows, Vol. 66, 1995, pp. 99-105.
8. H. Masuda, A. Ebata, K. Teramae and N. Hishinuma, “Alteration of thermal conductivity and viscosity of liquid by dispersing ultra-fine particles”, Netsu Bussei, Vol. 7, 1993, pp. 227–233.
9. J. Buongiorno and W. Hu, “Nanofluid coolants for advanced nuclear power plants”, Paper no. 5705, Proceedings of ICAPP, 2005.
10. R. Iwatsu, J. M. Hyun and K. Kuwahara, “Mixed convection in a driven cavity with a stable temperature gradient”, Int. J. Heat and Mass Transfer, Vol. 36, 1993, pp. 1601–1608.
11. H. F. Oztop and I. Dagtekin, “Mixed convection in two-sided lid-driven differentially heated square cavity, Int. J. Heat and Mass Transfer”, Vol. 47, 2004, pp. 1761–1769.
12. J. J. Hwang, “Turbulent heat transfer and fluid flow in a porous-baffled channel”, J. Thermophys. Heat Transfer, Vol. 11, 1997, pp. 429–436.
13. Y. T. Yang and C. Z. Hwang, “Calculation of turbulent flow and heat transfer in a porous-baffled channel”, Int. J. Heat and Mass Transfer, Vol. 46, 2003, pp. 771–780.
14. C. Berner, F. Durst and D. M. McEligot, “Flow around baffles”, J. Heat Transfer, Vol. 106, 1984, pp. 743-749.
15. K. M. Kelkar and S. V. Patankar, “Numerical prediction of flow and heat transfer in a parallel plate channel with staggered fins”, J. Heat Transfer, Vol. 109, 1987, pp. 25–30.
16. B. W. Webb and S. Ramadhyani, “Conjugate heat transfer in a channel with staggered ribs”, Int. J. Heat and Mass Transfer, Vol. 28, 1985, pp. 1679–1687.
17. S. T. Tansmim and M. R. Collins, “Numerical analysis of heat transfer in a square cavity with a baffle on the hot wall”, Int. Commun. Heat and Mass Transfer, Vol. 31, 2004, pp. 639-650.
18. M. Sheikholeslami, Zahir Shah, Ahmad Shafee, Ilyas Khan, Iskander Tlili, “Uniform magnetic force impact on water based nanofluid thermal behavior in a porous enclosure with ellipse shaped obstacle”, Scientific reports, Vol. 9, 2019, pp. 1-11.
19. R. Andrzejczyk, T. Muszynski, “An experimental investigation on the effect of new continuous core-baffle geometry on the mixed convection heat transfer in shell and coil heat exchanger”, Applied Thermal Engineering, Vol. 136, 2018, pp. 237-251.
20. A. Abedini, T. Armaghani, Ali J. Chamkha, “MHD free convection heat transfer of a water–Fe3O4 nanofluid in a baffled C-shaped enclosure”, Journal of Thermal Analysis and Calorimetry, Vol. 135, 2018, pp. 685-695.


## AUTHORS PROFILE

**Dr. M. Karuna Prasad** completed M. Sc and Ph. D in Gulbarga University. He has more than 6 years teaching and research experience. He has life membership in Indian Society of Theoretical and Applied Mechanics as well as he presented research papers in National and International Conferences, and published research papers in peer reviewed Scopus indexed and UGC listed Journals. He awarded Project fellow under UGC-Major Research Project. He is expertise in Mathematical Flow modelling of real time processes. He is teaching Numerical Method, Fluid Mechanics, Algebra, Linear Transform Methods, Complex Analysis, Real analysis and Operational Research using various software like C, MATLAB and Mathematica.

**Prof. J. Prathap Kumar** received Doctoral Degree from Gulbarga University and published more than 60 research articles in peer reviewed Scopus indexed and UGC listed Journals. He guided around 10 Doctoral students. He completed UGC-Major Research Project and he has more than 20 years teaching and research experience in UG and PG. He has life membership in Indian Society of Theoretical and Applied Mechanics and others. He has given invited talks in National and International Conferences. He is teaching Numerical Method, Fluid Mechanics, Algebra, Linear Transform Methods, Complex Analysis, Real analysis and Operational Research using various software like C, MATLAB and Mathematica.

**Prof. J. C Umavathi** received Doctoral Degree from Gulbarga University and published more than 150 research articles in peer reviewed Scopus indexed, SCI and UGC listed Journals. She guided around 10 Doctoral students. She received **Young Scientist Award and J. C Bose Award** and she has more than **2000** citations. She completed UGC-Major Research Project and she has more than 20 years teaching and research experience in UG and PG. She has life membership in Indian Society of Theoretical and Applied Mechanics and others as well as given many invited talks in National and International Conferences. She is expertise in flow modelling with Mathematica and MATLAB software’s etc. https://scholar.google.co.in/citations?user=DSjweGoAAAAJ&hl=en

**Dr. B. Devika** completed M. Sc and Ph. D in Sri Venkateswara University. She has more than 8 years teaching and research experience. She has life membership in Andhra Pradesh Mathematical Society as well as she presented research papers in National and International Conferences, and attended several workshops. She published research papers in peer reviewed Scopus indexed and UGC listed Journals. She is expertise in Mathematical Flow modelling of real time processes. She is teaching Numerical Method, Fluid Mechanics, Algebra, Linear Transform Methods, Complex Analysis, Real analysis and Ordinary and Partial Differential Equations using various software like C, MATLAB and Mathematica.

**Dr. C.S.K. Raju**, completed doctorate from VIT University, Vellore. He has published around **120** research articles in peer reviewed Scopus/Sci Indexed/ UGC listed journals. He has been acting as Editorial Board member and reviewer for many well-known publishers Elsevier, Springer and ASME societies. He has received Best Teacher award from IJRULA association and Young Scientist award from VD Technology. He has life membership in IJRULA, Association of Mathematics Teacher of India (AMTI), IJRULA, Indian Science Congress and International Association of Engineers. He has more than **1100 Scopus** citations. He has presented and given invited talk at National and International Conferences. For further reference go through the links: http://drchakravarthula.ga/index.html.